RESONATOR-BASED METERING OF POWER COMPONENTS ACCORDING TO IEEE STANDARD 1459-2010
MERENJE SNAGE PO STANDARDU IEEE 1459-2010 UPOTREBOM REZONATORSKIH FILTERSKIH STRUKTURA

Miodrag KUŠLJEVIĆ*, Josif TOMIĆ**, Predrag POLJAK***,
*Termoelektro Enel AD, 11010 Belgrade, Bačvanska 21/III, Serbia
**Faculty of Technical Sciences, 21000 Novi Sad, Trg Dositeja Obradovića 6, Serbia
***Institute of Chemistry, Technology and Metallurgy, 11000 Belgrade, Njegoševa 12, Serbia
e-mail: Miodrag.Kusljevic@te-enel.rs

ABSTRACT

This paper proposes an accurate and computationally efficient implementation of the IEEE Std. 1459-2010 for power measurements. An implementation is based on digital resonators embedded in a feedback loop. In the first algorithm stage, the unknown signal harmonic parameters are estimated. By this, the voltage and current signals are processed independently of each other. In the second algorithm stage, the unknown power components are estimated (calculated) based on estimated spectra. To demonstrate the performance of the developed algorithm, computer-simulated data and laboratory testing records are processed. Simple LabView implementation, based on the point-by-point processing feature, demonstrates techniques modest computation requirements and confirms that the proposed algorithm is suitable for real-time applications.

Keywords: IEEE Standard 1459–2010, power quality (PQ), power measurement, harmonic analysis, recursive algorithm, adaptive filtering, resonator filters, decimation filters, finite-impulse-response (FIR) filter, virtual instrument (VI), real-time system, point-by-point analysis.

REZIME

Liberalizacijom tržišta električne energije merenje električne snage i energije u nesinusoidalnim uslovima dobilo je veliki značaj. Ta tema je još uvek predmet aktivnih rasprava, tako da ne postoji neka generalizovana teorija koja se može uzeti kao osnova za potrebe obračuna, evaluacije kvaliteta energije, detekcije izvora harmonika i kompenzacije u energetskim sistemima. Kao posledica, postojeći standardi se odnose na sinusoidalne slučajeve i ne daju definiciju reaktivne energije (i/ili snage) u nesinusoidalnim uslovima. Slično, oni ne daju specifične zahteve za tačnost i odgovarajuće uslove testiranja u prisustvu harmonijskih izobličenja. Jedini standard koji se odnosi na ovu problematiku je IEEE Std. 1459–2010 koji ne daje definiciju reaktivne snage u nesinusoidalnim uslovima. Koncept ovog IEEE standarda je baziran na razdvajanju snage na fundamentalni i nefundamentalni deo. Ovaj prilaz separacije na fundamentalni i harmonijski deo može se primeniti na najbitnije veličine i može se iskoristiti kao indikator kvaliteta.

U radu je prikazana jedna efikasna algoritamska struktura za računanje električnih veličina definisanih standardom IEEE 1459-2010. Struktura se sastoji od dva dekuplovana dela. Za estimaciju spektra napona i struje korišćena je efikasna metoda bazirana na paralelnoj strukturi rezonantnih filtera sa zajedničkom povratnom vezom. U drugom delu strukture se na osnovu poznatog spektra naponskog i strujnog signala računaju komponente snage i indikatori kvaliteta na osnovu definicija datih u standardu IEEE 1459-2010. Predloženi algoritam je pogodan za primene u realnom vremenu. Realizacijom virtualnog instrumenta baziranog na PC računaru i programskom paketu LabVIEW, u cilju procene performansi algoritma, izvršene su računarske simulacije i eksperimentalna merenja i dati njihovi rezultati.

Ključne reči: Standard IEEE 1459–2010, kvalitet energije (PQ), merenje snage, harmonijska analiza, rekurzivni algoritam, adaptivno filtriranje, rezonantni filteri, decimacioni filteri, filter sa konačnim impulsnim odzivom (FIR filter), virtualni instrument (VI), real-time sistem, point-by-point analiza.

INTRODUCTION

With the liberalization of the electricity market, the measurement of electricity and energy in non-sinusoidal conditions has gained great importance. This topic is still the subject of active discussions, so there is no generalized theory that can be taken as a basis for the purposes of calculation, evaluation of energy quality, detection of harmonic sources and compensation in energy systems. As a consequence, existing standards apply to sinusoidal cases and do not provide a definition of reactive energy (or power) in non-sinusoidal conditions *(Cataliotti et al., 2009; Emanuel, 2010)*. Similarly, they do not give specific requirements for accuracy and appropriate test conditions in the presence of harmonic distortions. The only standard related to this issue is IEEE Std. 1459–2010 *(IEEE Std 1459-2010, 2010)*, which does not provide a definition of reactive

power in non-sinusoidal conditions. The concept of this IEEE standard is based on the separation of power into fundamental and non-fundamental parts. This approach of separation to the fundamental and harmonic part can be applied to the most important quantities and can be used as an indicator of quality.

Various techniques for the implementation of IEEE Std standards are present in the literature. 1459–2010. This standard is implemented using two basic approaches: (1) a two-step algorithm with an estimation of harmonic spectra of voltage and current signal in the first step and calculation of unknown power components in the second step, *(Chen, 2013; Gherasim et al., 2004; Terzija et al., 2007; Tomic et al., 2010)*, and (2) filter implementation combined with Clarke – Park transformation in the case of a three-phase system *(Cataliotti et al., 2008; Emanuel & Milanez, 2006; Pigazo & Moreno, 2007; Poljak et al., 2012)*.

If the implementation of the standard is done on the basis of the first approach, it is necessary to know the values of harmonics,

but the standard itself does not specify which method is used for harmonic signal analysis. Several algorithms for harmonic analysis are present in the literature. Fast Fourier Transform (FFT) is a numerically efficient algorithm for calculating Discrete Fourier Transform (DFT) and is the most commonly used algorithm for harmonic analysis *(Gherasim et al., 2004; IJ & S Loureiro, 2015)*. However, FFT also has the bad property of requiring synchronization of the sampling frequency with the signal frequency. In cases when this condition is not met, there are aliasing effects, leakage effect and picket-fence effect. There are various methods in the literature for the correction of these deficiencies, for example, time weight functions are used, the so-called windows, interpolation of DFT coefficients, etc.

In addition to the disadvantages related to the need to synchronize the sampling rate with the signal frequency, FFT has disadvantages caused by the block implementation. Namely, FFT processes a complete block of data and cannot give results for time moments inside a window. If the processing is performed in the so-called slide mode, i.e. if FFT is applied successively to windows shifted by one step, a much larger volume of computational operations is required.

A numerical algorithm that treats the frequency of a system as an unknown parameter of a mathematical model and estimates it together with other parameters of the input signals is presented in *(Terzija et al., 2007)*. In this way, the problem of sensitivity of measurements to frequency variations in a wide range is solved. By including the frequency in the vector of unknown parameters of the mathematical model, the model became nonlinear, which requires the application of nonlinear estimation techniques, so the algorithm is numerically intensive and therefore not suitable for real-time application.

In the works *(Kusljevic, 2010; Yang et al., 2005)*, a method based on adaptive filtering using a finite-impulse response filter (FIR) was applied, which avoids problems related to synchronizing the sampling frequency with the signal frequency. However, the amount of computation required has increased compared to FFT, so the algorithm does not meet the requirements of online implementations.

The paper *(Tomic et al., 2010)* presents an efficient method for measuring electrical quantities and electricity quality indicators defined by the IEEE 1459-2010 standard. The presented method does not require strict periodicity and does not require the use of window functions and/or synchronization with the fundamental component. The algorithm is based on general form for recursive discrete transformations for the realization of FIR and IIR filter transfer functions in order to avoid the shortcomings of the above algorithms. The algorithm structure is based on digital parallel resonant filters with common feedback.

The method proposed in this paper represents an improved technique used in *(Tomic et al., 2010)*. In this paper, improvements using oversampling and decimation filter techniques applied in *(Kusljevic, 2010)* were used. The serial connection of antialiasing of low-pass filters and FIR comb filters of a lower order, whose input signal is obtained by the decimation of the signal from the output of the low-pass filter, avoids problems related to sensitivity to rounding coefficients, reduces the scope of numerical calculations and increases frequency measurement accuracy.

MATERIAL

Basic Definitions of IEEE Standard 1459-2010

Assume that voltage and current are defined by the following time functions:

$$v(t) = V_0 + \sqrt{2} \sum_{h\neq0}^{\infty} V_h \sin(h\omega_1 t + \alpha_h) \quad (1)$$

$$i(t) = I_0 + \sqrt{2} \sum_{h\neq0}^{\infty} I_h \sin(h\omega_1 t + \beta_h) \quad (2)$$

where $v(t)$ and $i(t)$ are the instantaneous voltage and current, V_0 and I_0 are their dc components, V_h and I_h, $h > 1$, are their harmonic components, V_1 and I_1 are their fundamental components. V_h and I_h, are the RMS values of voltage and current harmonic h, and α_h and β_h are the phase angles of voltage and current harmonic h, respectively. V_1 and I_1 are the RMS values of voltage and current fundamental components, and α_1 and β_1 are the phase angles of voltage and current fundamental components, respectively. $\omega_1 = 2\pi f_1$, f_1 is the fundamental frequency.

The basic idea of the IEEE standard 1459-2010 consists of dividing the power into basic (fundamental) and remaining (non-fundamental) parts. The respective RMS voltages and currents are:

$$V^2 = V_1^2 + V_H^2; \quad I^2 = I_1^2 + I_H^2 \quad (3)$$
where
$$V_H^2 = \sum_{h\neq1} V_h^2, I_H^2 = \sum_{h\neq1} I_h^2.$$
The total apparent power is:
$$S = VI \quad (4)$$

As a result of dividing the RMS value of current or voltage into 50 Hz (fundamental) and non-50 Hz parts, the apparent power can be expressed as follows:

$$S^2 = S_1^2 + S_N^2 \quad (5)$$
where S_1 and S_N are defined as fundamental and nonfundamental apparent power.

$$S_1^2 = (V_1 I_1)^2 = P_1^2 + Q_1^2 \quad (6)$$
where
$$P_1 = V_1 I_1 \cos\varphi_1, Q_1 = V_1 I_1 \sin\varphi_1.$$

φ_1 is the phase shift between the voltage and current signals of the fundamental component. Nonfundamental apparent power caused by harmonic distortions produced or absorbed by consumers consists of three components:

$$S_N^2 = D_I^2 + D_V^2 + S_H^2 = (V_1 I_H)^2 + (V_H I_1)^2 + (V_H I_H)^2 \quad (7)$$

The first component, the current distortion power D_I, represents the increase in power due to current distortion when the voltage source is ideally sinusoidal and it is usually the dominant component. The second component, voltage distortion power D_V, is an effect caused by voltage distortion at the busbars. The third component, the harmonic apparent power S_H, represents the power obtained by multiplying the harmonics of voltage and current. It can be further divided into total harmonic active power and total harmonic nonactive power *(IEEE Std 1459-2010, 2010)*:

$$S_H^2 = (V_H I_H)^2 = P_H^2 + N_H^2 \quad (8)$$
where $P_H = P - P_1 = \sum_{h\neq1} V_h I_h \cos\varphi_h$
φ_h is the phase shift between the voltage and current harmonic h.

Each component of nonfundamental apparent power can be obtained by total harmonic distortion (THD) of voltage and/or current. THD is defined as the quotient of the RMS values of the higher harmonics and the RMS values of the fundamental harmonics. THD currents and THD voltages are:

$$THD_I = I_H/I_1, THD_V = V_H/V_1 . \quad (9)$$
It follows:
$$D_I = THD_I S_1, D_V = THD_V S_1, S_H = THD_I THD_V S_1. \quad (10)$$
The total nonactive power N is defined as follows:
$$N^2 = S^2 - P^2. \quad (11)$$
The power factor is defined as the ratio of active power to apparent power:
$$PF = P/S = (P_1 + P_H)/S \quad (12)$$

METHOD

Harmonic Analysis

The block diagram of the structure is shown in Fig. 1. The structure is based on discrete resonant filters with common feedback.

Resonant Filter Structure

Not so long ago, a general form based on the signal model was recommended for the implementation of recursive discrete transformations, which proved to be suitable for all filter signal processing, especially for the realization of DFT. The form and its parameters were arrived at on the basis of the formulation in the state space and the results of the estimation theory. The structure is nothing but an estimator that uses the signal model being measured *(Hostetter, 1980; Péceli, 1986)*.

Although the resonant filters with multiple poles provide better features related to nonstationary signals *(Kusljevic et al., 2017)*, for sake of simplicity, the case of a resonant filter with multiple poles has not been considered, so that each channel of the parallel structure contains elements with discrete transfer functions:

$$H_m(z) = \frac{r_m z^{-1}}{1 - z_m z^{-1}}, \ m = -M, \dots, 0, \dots, M, \ M\omega_1 < \pi, \quad (13)$$

where $z^{-1} = e^{-j2\pi f/f_s}$, $z_m = e^{j2\pi m f_1/f_s}$, f_s is a sampling rate, $T = 1/f_s$, $\omega = 2\pi f$.
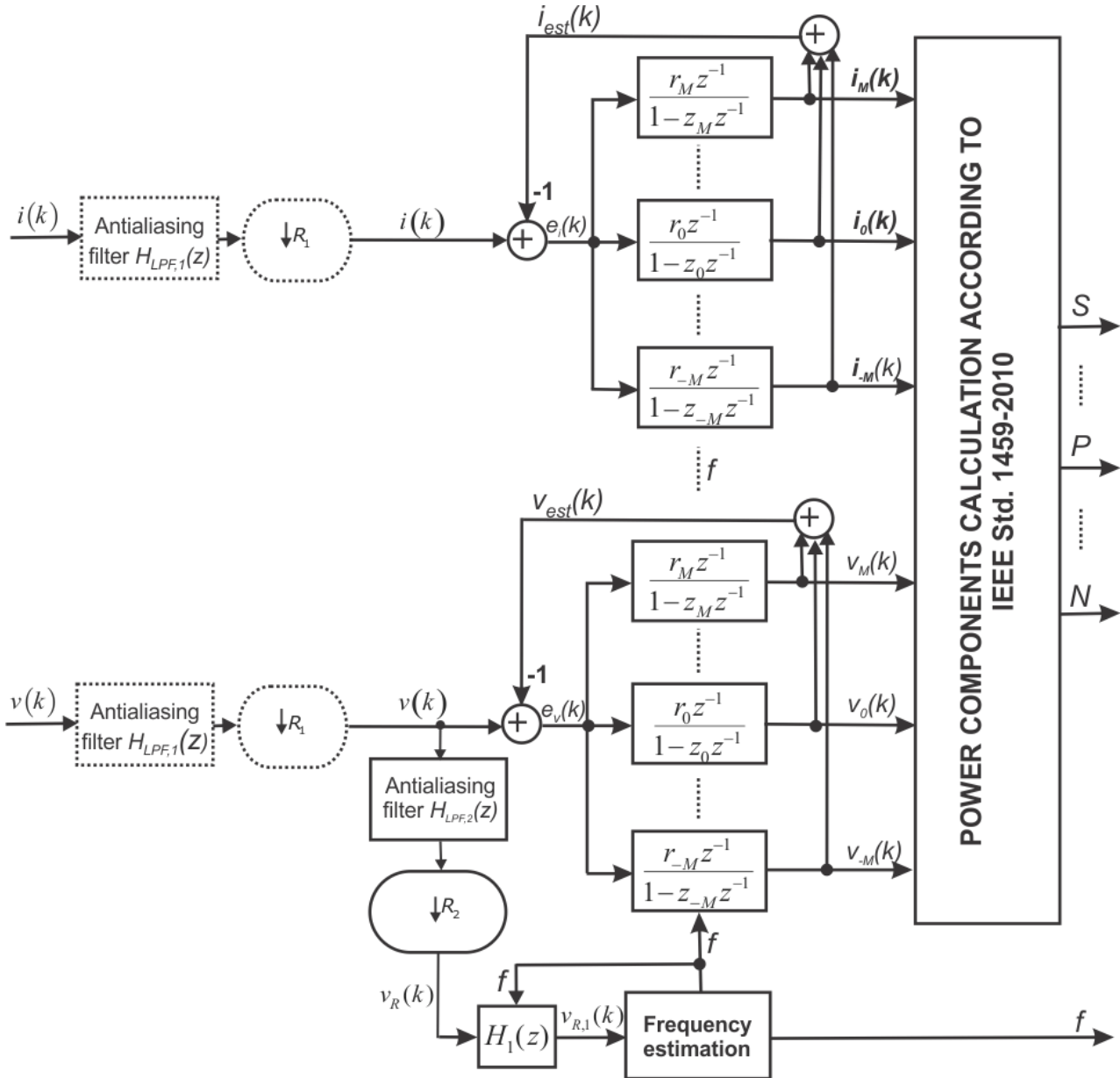

Fig. 1. Block diagram of the resonant filter strukture and estimator

Discrete transfer functions (13) are usually functions of complex coefficients and have poles on the unit circle. It is assumed that the poles and zeros are real numbers or that they appear as pairs of conjugate complex numbers, i.e. $z_m = z_{-m}^*$.

The resulting discrete transfer function for a channel m is

$$T_m(z) = \frac{H_m(z)}{1 + \sum_{n=-M}^{M} H_n(z)}, \ m = -M, \dots, 0, \dots, M. \quad (14)$$

An interesting feature of this structure is:

$$T_m(z_n) = \begin{cases} 1 & for \quad n = m \\ 0 & for \quad n \neq m \end{cases}$$

$$m = -M, \dots, 0, \dots, M, \ n = -M, \dots, 0, \dots, M \quad (15)$$

from which it can be concluded that the sensitivity of the transfer function in $z = z_m$, $m = -M, \dots, 0, \dots, M$, in relation to any $H_n(z)$ and z_n $(n = -M, \dots, 0, \dots, M)$, equals to zero, except in case of $n = m$.

It is important to note that this general feedback form provides an ideal pole-zero cancellation mechanism. This property is a consequence of the infinite gain of the feedback in the frequencies corresponding to the given poles, which enables absolute independence from the coefficients within the feedback loop. This is why the application of ideal resonant filters does not cause problems during implementation, since each pole is canceled by the zero, generated by the common feedback. This is true even in cases where rounding errors occur.

Calculating the parameters for such a structure is extremely simple. If the positions of the resonant filters $\{z_m\}$, $m = -M, \ldots, 0, \ldots, M$, are known and if $\{p_n\}$, $n = 0, 1, \ldots, N - 1$, are given poles of the filter, then, *(Péceli, 1986)*:

$$r_m = z_m \frac{\prod_{n=0}^{N-1}(1-p_n z_m^{-1})}{\prod_{\substack{n=-M\\n\neq m}}^{M}(1-z_n z_m^{-1})}, m = \text{-}M, \ldots, 0, \ldots, M \quad (16)$$

For a dead-beat observer, the parameters can be calculated as follows:

$$r_m = \frac{z_m^{2M+1}}{\prod_{\substack{n=-M\\n\neq m}}^{M}(z_m - z_n)}, m = \text{-}M, \ldots, 0, \ldots, M \quad (17)$$

The amplitude and phase of the *m*th voltage and current harmonics are calculated using the outputs of the resonant filter. For example, for the *m*th voltage harmonic at moment *k* is valid:

$$V_m(k) = \sqrt{(\text{Re } v_m(k))^2 + (\text{Im } v_m(k))^2},$$
$$\varphi_m(k) = \arctan \frac{\text{Im } v_m(k)}{\text{Re } v_m(k)} \quad (18)$$

It is necessary to calculate only one-half of the components since the other half represents their mirror image.

Frequency Measurement

Since the fundamental frequency is not constant, it is necessary to calculate the filter coefficients during the measurement. In *(Kusljevic, 2010; Tomic et al., 2010)*, an external module was used to estimate the frequency which is further used to calculate the coefficients (15) and (16), respectively. A closed form for calculating FIR filter coefficients for a known frequency is given. The method basically consists of the synthesis of second-order FIR subsections that should eliminate the dc component and unwanted higher harmonics, and have a unit gain for the desired harmonic. The complete filter is realized as a cascade of these modules.

However, although this combined structure has shown good convergence and estimation accuracy, the FIR filters in the frequency estimation module show limitations in the sensitivity of the coefficients during implementation, so that inadmissible errors occur for higher-order FIR filters, even for cascades of 30 second-order subsections, i.e. 60-order FIR filter. It should be mentioned that slightly better results are obtained if the order of subsections in the cascade is chosen at random. On the other hand, low-pass filters cannot effectively eliminate all harmonics if higher-order filters are not used, which again undesirably increases the convergence time. Good characteristics can be achieved by serial connection of an antialiasing low-pass filter with a sufficiently wide bandwidth (up to 8-16 harmonics) to ensure fast response and a lower-order FIR filter whose signal input is obtained by the decimation of the signal from the low-pass filter output. In this way, problems with the sensitivity of the coefficients are avoided, the scope of numerical calculations is reduced and the accuracy of frequency measurements is increased. Cascaded integrator-comb (CIC) filters can be used as antialiasing filters *(Lyons, 2014)*

$$H_{CIC}(z) = \left(\frac{1}{D}\frac{1-z^{-D}}{1-z^{-1}}\right)^S. \quad (19)$$

These filters are also called *SincS* filters because their amplitude characteristic corresponds to the function $Sinc(x) = \sin x/x$. Their advantage is reflected in the simple implementation.

The output of the filter (19) leads to the input of the FIR filter whose sampling frequency is reduced by a factor of *R*. The FIR filter which eliminates the dc component and the frequency $\omega_S/2R$ and has a unit gain for the fundamental frequency ω_1 has the following form:

$$H_{10}(z) = \frac{1-z^{-2R}}{|1-z_1^{-2R}|}, \; |1 - z_1^{-2R}| = 2\sin(\omega_1 RT). \quad (20)$$

where $z^{-1} = e^{-j2\pi f/fs}$ and $z_1^{-1} = e^{-j2\pi f_1/fs}$.

A second-order FIR filter that eliminates the harmonic ω_i and has a unit gain for the fundamental frequency ω_1 has the form

$$H_{1i}(z) = \frac{1 - 2\cos(\omega_i RT)z^{-R} + z^{-2R}}{|1 - 2\cos(\omega_i RT)z_1^{-R} + z_1^{-2R}|}, \quad (21)$$

$|1 - 2\cos(\omega_i RT)z_1^{-R} + z_1^{-2R}| = 2|\cos(\omega_1 RT) - \cos(i\omega_1 RT)|$, $i = 2, 3, \ldots, [M/R]$, where $[M/R]$ denotes maximum integer part of M/R and is equal to the number of elements in the cascade.

$$H_1(z) = H_{10}(z) \prod_{i=2}^{[M/R]} H_{1i}(z). \quad (22)$$

Fig. 2 shows the amplitude-frequency characteristics of CIC and FIR filters and their cascade for $f_s = 6.4$ kHz, $D = 8$, $S = 3$. $R = 4$, $f_1 = 49.8$ Hz.

A large number of algorithms for measuring the frequency of alternating signals have been described in the literature. Newer recursive methods based on three consecutive signal samples are described in *(Kusljevic, 2010; Kušljević et al., 2010; Yang et al., 2005)*. Three consecutive samples of the basic component of the signal $v_{R,1}(k)$ obtained by filtering the signal (1) and reducing the sampling frequency with the factor *R*, at time instant *k* are related to the following linear relation:

$$y(k) = z(k)x(k) \quad (23)$$

where $y(k) = [v_{R,1}(k) + v_{R,1}(k-2)]/2$, $z(k) = v_{R,1}(k-1)$, $x(k) = \cos(\omega_1 RT)$.

After estimating the parameter *x(k)*, the frequency is determined by

$$f(k) = \arccos(x(k))/(2\pi RT) \quad (24)$$

In the case when the frequency is calculated directly by (23), large errors can occur when the samples are close to the signal passing through zero, due to the final word length resolution or due to the presence of noise. In (Yang et al., 2005), in order to increase the performance of the algorithm, the problem of parameter estimation was transformed into a predetermined system of linear equations to which the LS algorithm was applied. Similarly, a weighted-least-square (WLS) algorithm with a suitable procedure for adjusting the forgetting (transition) factor was used in *(Kušljević et al., 2010; Tomic et al., 2010)*. The WLS algorithm was also used in this paper.

Incorrect data corresponding to poor frequency estimates are identified and eliminated by median filters. Unlike the median filter, linear filters take into account all data, including bad ones, when calculating the output. Another advantage of a median filter is that it is not necessary to specify a cut-off frequency.
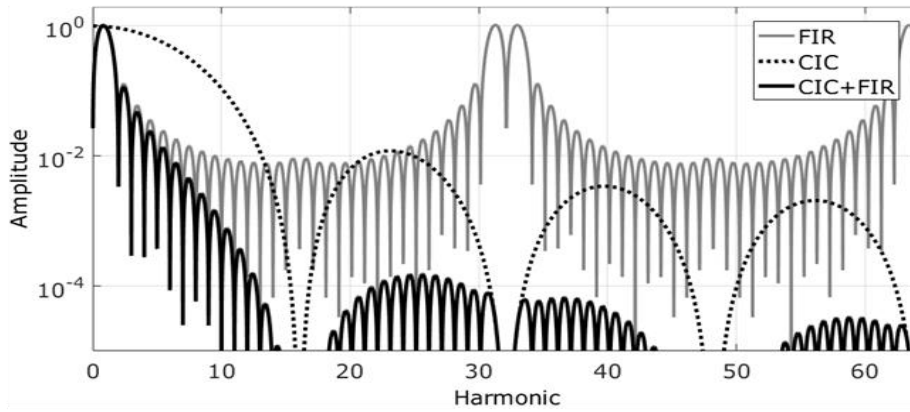
Fig. 2. Frequency responses of the fundamental component filter for the fundamental frequency
$f_1 = 49.8$ Hz *and the sampling frequency* $f_s = 6.4$ kHz *and* $D = 8$, $S = 3$, $R = 4$.

RESULTS AND DISCUSSION

Simulation Results

The time responses of the described algorithm for the step change of the fundamental harmonic amplitude from 1 to 0.9 p.u. (with a fixed frequency of 50 Hz) and the step frequency change from 50 Hz to 49.8 Hz are shown in Fig. 3 and Fig. 4, respectively. Additive white Gaussian noise of zero mean value with SNR=60 dB and the third and fifth harmonics with 30% and 10% of the fundamental harmonic, respectively, were present in the signal. The sampling frequency is $f_s = 6.4$ kHz. The following parameters were used in the frequency estimation module for the antialiasing CIC filter: $D_2 = 8$ and $S_2 = 3$. The reduction factor $R_2 = 4$ was used.

In the first case, the proposed algorithm and FFT after the convergence period give identical responses, while in the second case (when the synchronization condition is not met) the proposed algorithm shows superiority over FFT. Fluctuations of the measured value around the exact value are a consequence of the presence of noise in the input signal. If better accuracy were to be achieved, the effect of the presence of noise could be reduced by introducing the poles into the resonant structure transfer function. However, it should be emphasized that this comes down to additional filtering of the input signal which prolongs the convergence time.

In the second test, the sensitivity of the algorithm to random noise, present in the processed signal, was analyzed. Additive noise, amplitudes distributed according to the Gaussian distribution, was added to the processed simple periodic signal of constant frequency in the range of 30-70 Hz. Fig. 5 shows the maximum errors in the estimation of power components at a time interval of 5 seconds depending on the SNR.
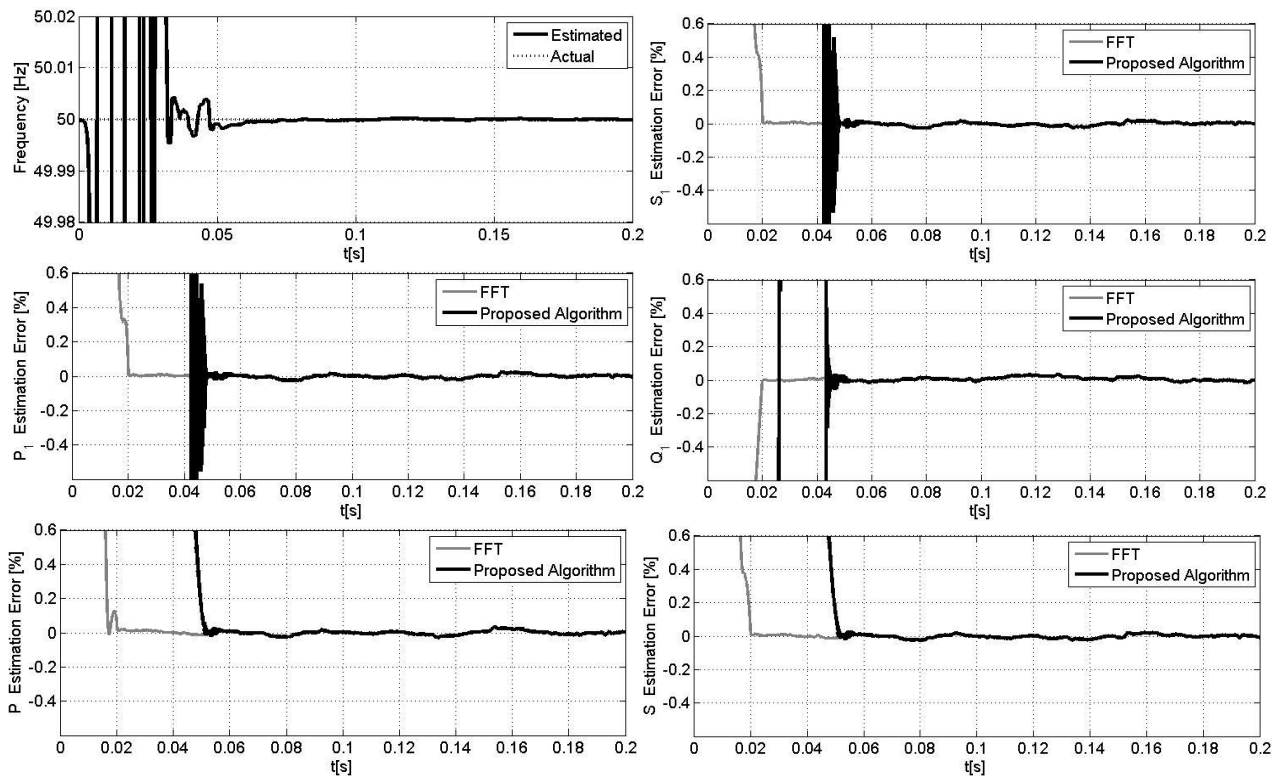

Fig. 3. Estimation errors for f=50 Hz and $V_1= I_1=1$ p.u. for t<0s and $V_1= I_1=0.9$ p.u. for t>0s, with SNR=60 dB and with harmonics presence

No input antialiasing filter and sampling frequency reduction ($H_{\mathrm{LPF},1}(z) = 1$, $R_1 = 1$) were used. In cases where the Signal-to-Noise-Ratio (SNR) is low, the accuracy of the algorithm can be further improved by oversampling the input signals and antialiasing filters with a reduction of the sampling frequency, i.e. interpolation with antialiasing filters *(Lyons, 2014)*. Oversampling is a popular technique used in the DSP industry to increase the resolution of analog-to-digital conversion (ADC). Oversampling uses a sampling frequency that is much higher than Nyquist's one. This reduces the level of ADC noise with the possibility of further processing so that better ADC resolution is enabled. Each doubling of the sampling frequency increases the resolution by half a bit and reduces the noise level by 3 dB *(Tan & Jiang, 2018)*.
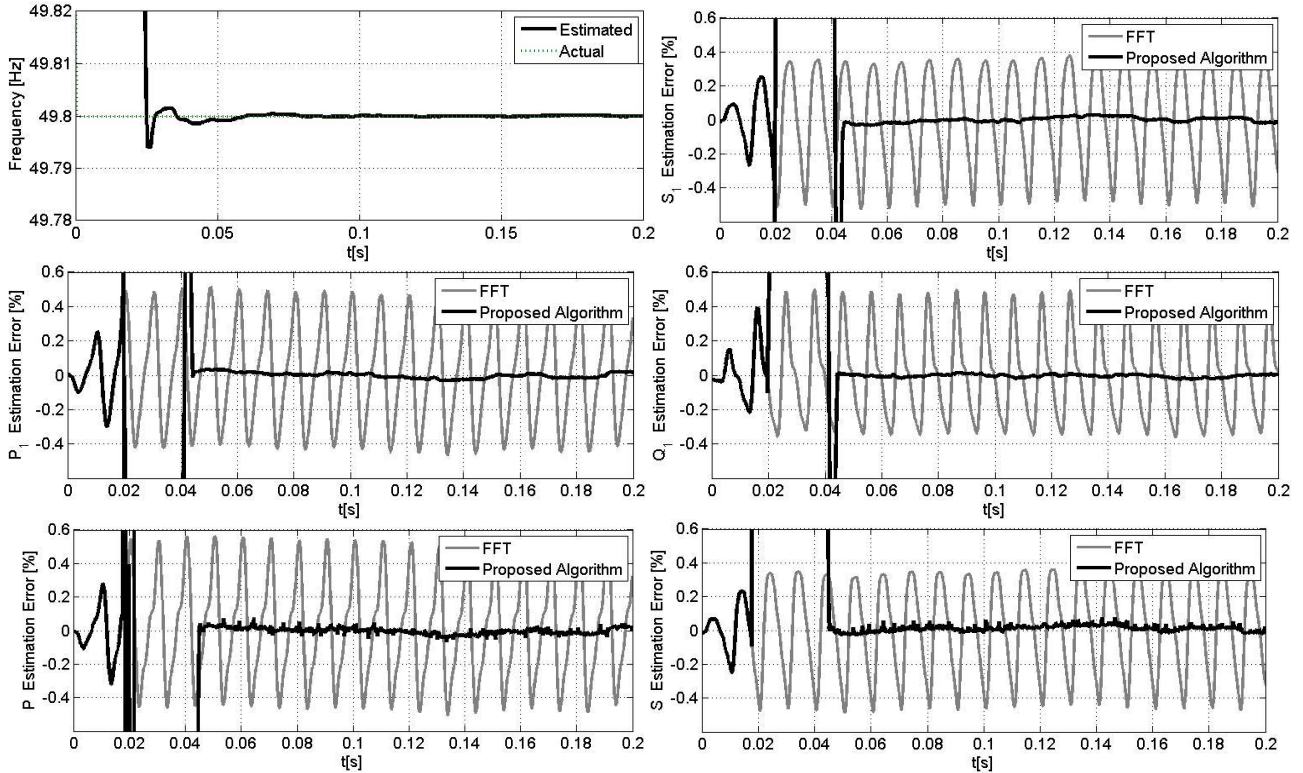

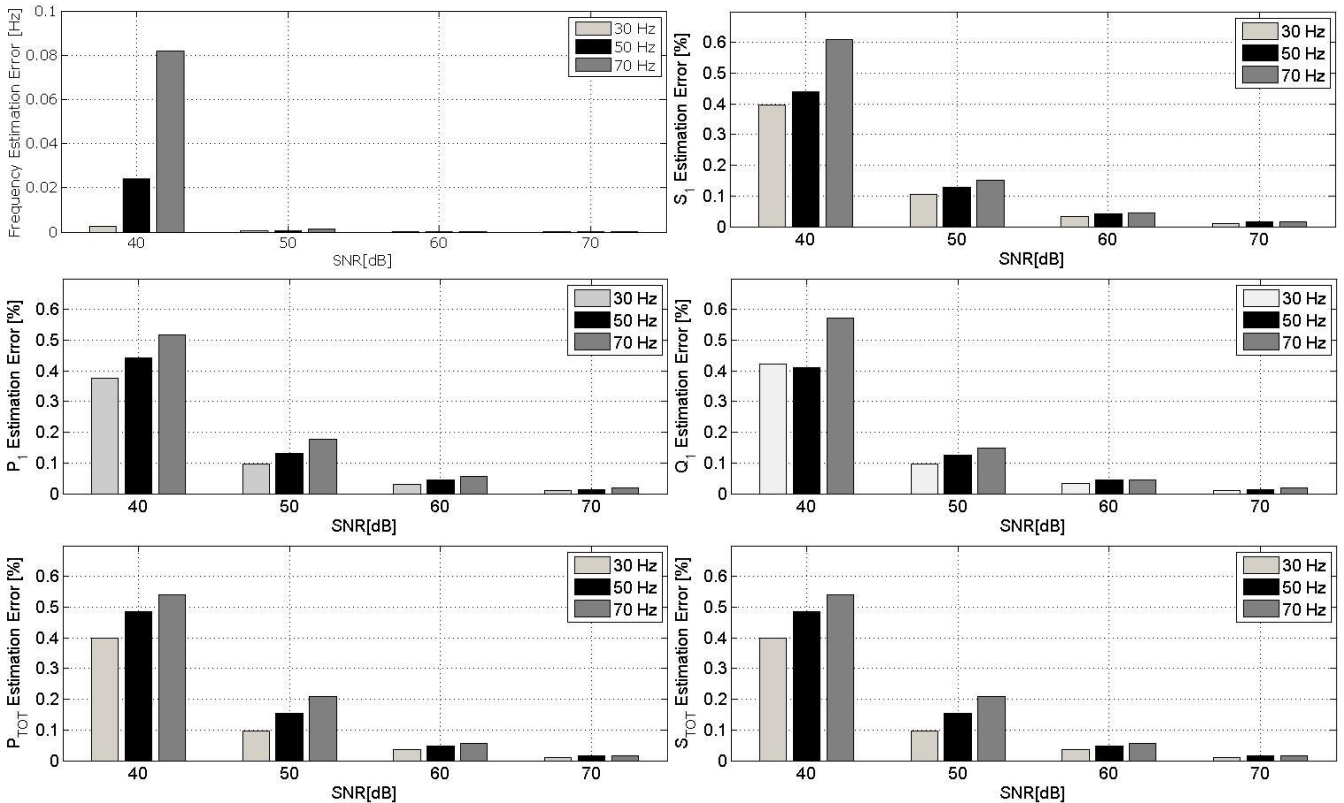Fig. 4. Estimations for f=50 Hz for t<0s and f=49,8 Hz for t>0s, with SNR=60 dB and with harmonics presence.

Fig. 5. Maximum estimation errors for noisy input signals.

Results of Experiments

In this section, the measurement results obtained using the realized prototype measuring system are presented. The system is based on the PC platform, the PCI-6221 acquisition card and the NI LabVIEW software package. The use of such a structure significantly reduces the time required to evaluate the method. The LabVIEW programming environment is very suitable for program development using a graphical programming language. LabVIEW also enables analysis and mathematical routines that are executed together with acquisition and visualization functions, so that they can be easily incorporated into any application. Further, LabVIEW supports point-by-point execution routines; these routines were developed to meet the needs of online analysis in real-time applications (*Real-Time Tutorial*, n.d.; Tools, 2001).

A point-by-point analysis is important to allow to control processes where there is a very fast, deterministic, point-by-point data acquisition. The point-by-point approach simplifies the design, implementation and testing process, enabling a flow that matches the data flow in the monitoring and management process, without the need for field allocation (*Real-Time Tutorial*, n.d.). As the name suggests, point-by-point processing is of the scalar type. It is suitable for real-time processing such as signal filtering as it allows input and output synchronization (*Kehtarnavaz & Kim, 2005*). With flow, stable point-by-point analysis, acquisition and process analysis can be brought closer to control processes using special circuits such as Field Programmable Gate Array (FPGA) chips.

The implemented acquisition system uses the standard NI PCI-6221 acquisition card. Its main features are 16 analog inputs, 16-bit resolution, a sampling rate of 250 ksamples/s and a very fast Direct Memory Access (DMA) channel. A standard PC with AMD Athlon (tm) 64 X2 Dual Core Processor 4800+ was used for signal processing. The measuring system uses Hall effect transducers, voltage transducers (LEM LV25-P with a response time $40\mu s$ and 0.8% accuracy) and a current sensor (LEM LA25-NP with a DC-150 kHz bandwidth and 0.5% accuracy), to generate a signal for a PCI card.

In order to evaluate the accuracy of the realized instrument, a voltage and current software generator was implemented using the LabVIEW software package and the NI PCI-6221 card. Voltage and current signals of known harmonic content were generated and converted to analog signals using 16-bit DACs. They were then sampled using 16-bit ADC instruments with a sampling frequency $f_s = 6.4$ kHz. The following parameters were used in the frequency estimation module for the antialiasing CIC filter: $D_2 = 8$ and $S_2 = 3$. The reduction factor $R_2 = 4$ was selected.

In the first step, voltage and current sensors were not used to determine the uncertainty related to the instrument itself, as the main contribution to the overall uncertainty comes from the sensors (*Cataliotti et al., 2008*). By the way, the main topic of this paper is the measurement algorithm. Measurements were performed for different cases, where the fundamental frequency of the generated signals was changed in the range of 30-70 Hz, with different harmonic content. Instrument testing was also performed using a fundamental component to which multiple harmonic components were added in accordance with Table I taken from (*Cataliotti et al., 2008*). Notice the amplitudes and phase shifts of voltage and current, for five equidistant points, from the sinusoidal condition to the maximum harmonic content.

As there are no other references related to the accuracy of measuring power components according to IEEE Std. 1459 (*Cataliotti et al., 2008*), the requirements of IEC Standard 61000-4-7 (*International Electrotechnical Commission, 2003*) were used as a reference for determining power components (active and non-active). IEC Standard 61000-4-7 for measuring harmonic components provides specific requirements for the maximum permissible errors of voltage, current and harmonic power. The total permissible power measurement error for Class I instruments is equal to $\pm 1\%$ when the measured power is greater than 150 W and ± 1.5 W for the measured power less than 150 W. It should be noted that these maximum permissible errors refer to pure sinusoidal and stationary signals, in the operating frequency range, applied on instruments under nominal operating conditions.

Table 1 - Test Conditions. a) Fundamental Voltage: V₁= 230 V, Phase = 0⁰, Voltage Harmonic Content. b) Fundamental Current: I₁ = 5a, Phase = −47.11⁰ , Current Harmonic Content (Cataliotti et al., 2008)

a)

Test condition	THDv [%]	2nd harmonic		3rd harmonic		5th harmonic	
		Ampl. [%]	Phase [deg]	Ampl. [%]	Phase [deg]	Ampl. [%]	Phase [deg]
1 (Sinusoidal)	0	0		0		0	
2 (Distorted)	5	3		2.8		2.8	
3 (Distorted)	10	6	-120^0	5.6	-62.98^0	5.6	149.5^0
4 (Distorted)	15	9		8.3		8.3	
5 (Distorted)	20	12		11		11	

b)

Test condition	THDi [%]	2nd harmonic		3rd harmonic		5th harmonic	
		Ampl. [%]	Phase [deg]	Ampl. [%]	Phase [deg]	Ampl. [%]	Phase [deg]
1 (Sinusoidal)	0	0		0		0	
2 (Distorted)	10.8	2		10		3.5	
3 (Distorted)	21.6	4	15^0	20	91.90^0	7	137.5^0
4 (Distorted)	32.3	6		30		10.5	
5 (Distorted)	43.1	8		40		14	

Table 2 shows the maximum errors of the measured quantities for all conditions. The results show that the achieved uncertainty is very small and significantly below the limits of the standard (*International Electrotechnical Commission, 2003*) and in accordance with the results obtained through simulations. It should be noted that these uncertainties are negligible compared to those caused by the presence of sensors.

To take into account the effects of the transducers, voltages and currents with the rich harmonic contents were brought to the virtual instrument via voltage and current transducers. The experiments were performed using a Fluke 6100A Electrical Power Standard calibrator (with a frequency accuracy of 50 ppm, a frequency setting resolution of 0.1 Hz, a six-digit voltage/current amplitude resolution, the possibility of programming from one to four independent phases, completely independent voltage and current control in each phase, 1 kV and 20 A output for each phase, up to 100 harmonics simultaneously). The conditions defined in Table 1 were applied. The maximum errors for the measured power components and for all considered signals are shown in Table 2. It is obvious that the uncertainties introduced by the sensors are dominant in relation to the uncertainties of the implemented method, however, the total error of the virtual instrument with voltage and current transducers still does not exceed the limits of class I.

Table 2 – Maximum Measurement Errors

Quantity	Without Transducers			With Transducers		
	Total	Fundament.	Nonfundam.	Total	Fundament.	Nonfundam.
Voltage [V]	ε_V = 0.002%	ε_{V1} = 0.002%	ε_{VH} = 0.096%	ε_V = 0.004%	ε_{V1} = 0.004%	ε_{VH} = 0.160%
Current [A]	ε_I = 0.030%	ε_{I1} = 0.016%	ε_{IH} = 0.042%	ε_I = 0.200%	ε_{I1} = 0.130%	ε_{IH} = 0.820%
Apparent Power [VA]	ε_S =0.020%	ε_{SI}= 0.015%	ε_{SN} = 0.025% e_{SH} = 0.020 VA	ε_S = 0.022%	ε_{SI}= 0.100%	ε_{SN} = 0.910% e_{SH} = 0.310 VA
Active Power [W]	ε_P =0.060%	ε_{P1}= 0.070%	e_{PH}= 0.018 W	ε_P = 0.924%	ε_{P1}= 0.435	e_{PH} = 1.450 W
Nonactive Power [VAr]	ε_N =0.085%	ε_{QI}= 0.050%	e_{DI}= 0.028 VAr e_{DV}=0.028 VAr e_{DH}=0.015 VAr	ε_N =0.457%	ε_{QI}= 0.130%	e_{DI} =1.450 VAr e_{DV}= 0.580 VAr e_{DH} =1.330 VAr

CONCLUSION

The paper describes the structure and implementation of a new recursive method for measuring electrical quantities according to the IEEE Std standard. 1459-2010. The method has been tested in various conditions and found to be effective as a means of measuring electrical quantities. Simulation and experimental results have shown that the proposed technique allows accurate measurement and monitoring of changes in non-stationary conditions. Furthermore, the proposed technique is suitable for measurement in a wide range of frequency changes and the obtained results confirmed the good dynamic properties as well as the accuracy of the measurement. A simple LabVIEW implementation based on point-by-point processing has shown moderate requirements for computing resources and confirmed that the algorithm is suitable for real-time applications and for designing microprocessor devices that work in real-time and require precise and fast parameter measurement.

REFERENCES

Cataliotti, A., Cosentino, V., Lipari, A., & Nuccio, S. (2009). Metrological characterization and operating principle identification of static meters for reactive energy: An experimental approach under nonsinusoidal test conditions. IEEE Transactions on Instrumentation and Measurement, 58(5). https://doi.org/10.1109/TIM.2008.2009134

Cataliotti, A., Cosentino, V., & Nuccio, S. (2008). A virtual instrument for the measurement of IEEE Std. 1459-2000 power quantities. IEEE Transactions on Instrumentation and Measurement, 57(1). https://doi.org/10.1109/TIM.2007.908625

Chen, C. I. (2013). A two-stage solution procedure for digital power metering according to IEEE standard 1459-2010 in single-phase system. IEEE Transactions on Industrial Electronics, 60(12). https://doi.org/10.1109/TIE.2012.2228146

Emanuel, A. E. (2010). Power Definitions and the Physical Mechanism of Power Flow. In Power Definitions and the Physical Mechanism of Power Flow. https://doi.org/10.1002/9780470667149

Emanuel, A. E., & Milanez, D. L. (2006). Clarke's alpha, beta, and zero components: A possible approach for the conceptual design of instrumentation compatible with IEEE Std. 1459-2000. IEEE Transactions on Instrumentation and Measurement, 55(6), 2088–2095. https://doi.org/10.1109/TIM.2006.884125

Gherasim, C., van den Keybus, J., Driesen, J., & Belmans, R. (2004). DSP implementation of power measurements according to the IEEE trial-use Standard 1459. IEEE Transactions on Instrumentation and Measurement, 53(4), 1086–1092. https://doi.org/10.1109/TIM.2004.831509

Hostetter, G. H. (1980). Recursive Discrete Fourier Transformation. IEEE Transactions on Acoustics, Speech, and Signal Processing, 28(2). https://doi.org/10.1109/TASSP.1980.1163389

IEEE Std 1459-2010, 40 IEEE Std 1459-2010 (Revision of IEEE Std 1459-2000) (2010).

IJ, J. E., & S Loureiro, O. (2015). Research and Development of a Virtual Instrument for Measurement, Analysis and Monitoring of the Power Quality. Journal of Fundamentals of Renewable Energy and Applications, 05(05). https://doi.org/10.4172/2090-4541.1000185

International Electrotechnical Commission. (2003). Electromagnetic compatibility (EMC) Part 4-30: Testing and measurement techniques Power quality measurement methods. IEC Standard, 61000-4–30.

Kehtarnavaz, N., & Kim, N. (2005). Digital Signal Processing System-Level Design Using LabVIEW. In Digital Signal Processing System-Level Design Using LabVIEW. https://doi.org/10.1016/B978-0-7506-7914-5.X5000-4

Kusljevic, M. D. (2010). Simultaneous frequency and harmonic magnitude estimation using decoupled modules and multirate sampling. IEEE Transactions on Instrumentation and Measurement, 59(4). https://doi.org/10.1109/TIM.2009.2031426

Kušljević, M. D., Tomić, J. J., & Jovanović, L. D. (2010). Frequency estimation of three-phase power system using weighted-least- square algorithm and adaptive FIR filtering. IEEE Transactions on Instrumentation and Measurement, 59(2). https://doi.org/10.1109/TIM.2009.2023816

Kusljevic, M. D., Tomic, J. J., & Poljak, P. D. (2017). Maximally Flat-Frequency-Response Multiple-Resonator-Based Harmonic Analysis. IEEE Transactions on Instrumentation and Measurement, 66(12), 3387–3398. https://doi.org/10.1109/TIM.2017.2751799

Lyons, R. G. (2014). Understanding Digital Signal Processing Third Edition. In Vascular (Issue January 2010).

Péceli, G. (1986). A Common Structure for Recursive Discrete Transforms. IEEE Transactions on Circuits and Systems, 33(10). https://doi.org/10.1109/TCS.1986.1085844

Pigazo, A., & Moreno, V. M. (2007). Accurate and computationally efficient implementation of the IEEE 1459-2000 standard in three-phase three-wire power systems. IEEE Transactions on Power Delivery, 22(2). https://doi.org/10.1109/TPWRD.2006.881576

Poljak, P. D., Kuljevíc, M. D., & Tomíc, J. J. (2012). Power components estimation according to IEEE standard 1459-2010 under wide-range frequency deviations. IEEE Transactions on Instrumentation and Measurement, 61(3). https://doi.org/10.1109/TIM.2011.2171615

Real-Time Tutorial. (n.d.). http://www.ni.com/realtime

Tan, L., & Jiang, J. (2018). Digital signal processing: Fundamentals and applications. In Digital Signal Processing: Fundamentals and Applications. https://doi.org/10.1016/C2017-0-02319-4

Terzija, V. V., Stanojević, V., Popov, M., & van der Sluis, L. (2007). Digital metering of power components according to IEEE standard 1459-2000 using the Newton-type algorithm. IEEE Transactions on Instrumentation and Measurement, 56(6). https://doi.org/10.1109/TIM.2007.908235

Tomic, J. J., Kusljevic, M. D., & Marcetic, D. P. (2010). An adaptive resonator-based method for power measurements according to the IEEE trial-use standard 1459-2000. IEEE Transactions on Instrumentation and Measurement, 59(2). https://doi.org/10.1109/TIM.2009.2020840

Tools, I. (2001). Getting Started with LabVIEW. Building.

Yang, J. Z., Yu, C. S., & Liu, C. W. (2005). A new method for power signal harmonic analysis. IEEE Transactions on Power Delivery, 20(2 II), 1235–1239. https://doi.org/10.1109/TPWRD.2004.834311